

**EXPERIMENTAL ANALYSIS OF PERSPECTIVE
ELONGATION EFFECTS USING A LASER GUIDE
STAR IN AN ADAPTIVE-OPTICS SYSTEM:
POSTPRINT**

Kevin Vitayaudom, et. al

**Air Force Research Laboratory
3500 Aberdeen Ave SE
Kirtland AFB, NM 87117**

1 June 2009

Technical Paper

APPROVED FOR PUBLIC RELEASE; DISTRIBUTION IS UNLIMITED.



**AIR FORCE RESEARCH LABORATORY
Directed Energy Directorate
3550 Aberdeen Ave SE
AIR FORCE MATERIEL COMMAND
KIRTLAND AIR FORCE BASE, NM 87117-5776**

REPORT DOCUMENTATION PAGE

Form Approved
OMB No. 0704-0188

Public reporting burden for this collection of information is estimated to average 1 hour per response, including the time for reviewing instructions, searching existing data sources, gathering and maintaining the data needed, and completing and reviewing this collection of information. Send comments regarding this burden estimate or any other aspect of this collection of information, including suggestions for reducing this burden to Department of Defense, Washington Headquarters Services, Directorate for Information Operations and Reports (0704-0188), 1215 Jefferson Davis Highway, Suite 1204, Arlington, VA 22202-4302. Respondents should be aware that notwithstanding any other provision of law, no person shall be subject to any penalty for failing to comply with a collection of information if it does not display a currently valid OMB control number. **PLEASE DO NOT RETURN YOUR FORM TO THE ABOVE ADDRESS.**

1. REPORT DATE (DD-MM-YYYY) 01/06/2009		2. REPORT TYPE Technical Paper		3. DATES COVERED (From - To) October 1, 2008- June 1-2009	
4. TITLE AND SUBTITLE Experimental Analysis of Perspective Elongation Effects Using a Laser Guide Star in an Adaptive-Optics System: Post Print				5a. CONTRACT NUMBER In House DF702151	
				5b. GRANT NUMBER	
				5c. PROGRAM ELEMENT NUMBER 62890F	
6. AUTHOR(S) Kevin Vitayaudom, Darryl Sanchez, Denis Oesh*, Patrick Kelly, Carolyn Tewksbury-Christle, Julie Smith				5d. PROJECT NUMBER 2301	
				5e. TASK NUMBER SJ	
				5f. WORK UNIT NUMBER 41	
7. PERFORMING ORGANIZATION NAME(S) AND ADDRESS(ES) Air Force Research Laboratory 3550 Aberdeen Ave SE Kirtland AFB NM 87117				8. PERFORMING ORGANIZATION REPORT NUMBER *Science Applications International 2109 Airpark Road Southeast Albuquerque, NM 87106-3236	
9. SPONSORING / MONITORING AGENCY NAME(S) AND ADDRESS(ES) Air Force Research Laboratory 3550 Aberdeen Ave SE Kirtland AFB, NM 87117				10. SPONSOR/MONITOR'S ACRONYM(S) AFRL/RDSA	
				11. SPONSOR/MONITOR'S REPORT NUMBER(S) AFRL-RD-PS-TP-2010-1002	
12. DISTRIBUTION / AVAILABILITY STATEMENT Approved for public release					
13. SUPPLEMENTARY NOTES Accepted for publication in the SPIE Optics + Photonics; Titled: Optical Engineering + Applications; August 2-6, 2009; San Diego, CA. 377ABW-2009-0857; July 7, 09. "Government Purpose Rights"					
14. ABSTRACT The use of a laser guidestar (LGS) for the purpose of a beacon in an adaptive-optics (AO) system is prone to perspective elongation effects on the spots of a Shack-Hartmann wavefront sensor. The elongated spots can vary in size over the subapertures and affect the gradient sensitivity of the sensor. The Air Force Research Laboratory (AFRL) has developed a LGS model that outputs gradient gains which represent o the effects of an extended beacon on the spots for a Shack-Hartmann wavefront sensor. This paper investigates the application of these gains in an experimental setup in order to both analyze the effects of the variation in those gains due to spot size elongation and to measure the impact on the performance of an AO system.					
15. SUBJECT TERMS Adaptive Optics; Laser Guidestar; Sodium Beacon; Perspective Elongation; Centroid Gain Maps					
16. SECURITY CLASSIFICATION OF:			17. LIMITATION OF ABSTRACT	18. NUMBER OF PAGES	19a. NAME OF RESPONSIBLE PERSON Pat Kelly
a. REPORT Unclassified	b. ABSTRACT Unclassified	c. THIS PAGE Unclassified			19b. TELEPHONE NUMBER (include area code) 505- 846-2094

Standard Form 298 (Rev. 8-98)
Prescribed by ANSI Std. Z39.18

Experimental analysis of perspective elongation effects using a laser guide star in an adaptive-optics system

Kevin P. Vitayaudom^a, Darryl J. Sanchez^a, Denis W. Oesch^b, Patrick R. Kelly^a, Carolyn M. Tewksbury-Christle^a, and Julie C. Smith^a

^aAir Force Research Laboratory, 3550 Aberdeen Ave SE, Kirtland AFB, NM;

^bScience Applications International Corp., Albuquerque, NM

ABSTRACT

The use of a laser guidestar (LGS) for the purpose of a beacon in an adaptive-optics (AO) system is prone to perspective elongation effects on the spots of a Shack-Hartmann wavefront sensor. The elongated spots can vary in size over the subapertures and affect the gradient sensitivity of the sensor. The Air Force Research Laboratory (AFRL) has developed a LGS model that outputs gradient gains which represent the effects of an extended beacon on the spots for a Shack-Hartmann wavefront sensor. This paper investigates the application of these gains in an experimental setup in order to both analyze the effects of the variation in those gains due to spot size elongation and to measure the impact on the performance of an AO system.

Keywords: adaptive optics, laser guidestar, sodium beacon, perspective elongation, centroid gain maps

1. INTRODUCTION

The Atmospheric Simulation and Adaptive-Optics Laboratory Testbed (ASALT) at the Air Force Research Lab (AFRL), Starfire Optical Range (SOR), Kirtland Air Force base, New Mexico is beginning an investigation into setting up an optical bench with the capability of reproducing an extended beacon source. Before the extended source is placed on the optics testbed, initial experiments are being conducted on closed-loop performance of an adaptive-optics (AO) system that incorporates simulated effects of using an extended source. A model developed at the SOR outputs centroid gains that simulates perspective elongation effects of an extended beacon at different azimuth and elevation angles.¹ The simulated centroid gains from the model are applied to the outputted gradients from a Shack-Hartmann wavefront sensor (SH WFS) which is setup on an optical bench running closed-loop adaptive-optics operations.² These initial experiments are being used to gain insight into utilizing LGSs for adaptive-optics and expand our current testbed environment conditions to incorporate extended beacon effects. Once the testbed is retrofitted with the extended beacon source, the ASALT will conduct research on using extended beacons for adaptive-optics and to explore techniques for mitigating perspective elongation effects.

The astronomical community has proposed many different solutions for eliminating the effects of perspective elongation. Véran et al. explored the application of subaperture specific centroid gains in order to address the varied spot images on a SH WFS.³ The Keck observatory has also applied varied gradient biases on x and y subapertures to compensate for elongation effects that occur on their 10 m telescope. Research conducted in this paper will also apply subaperture specific centroid gains, but these gains will be representative of the degradation of WFS measurements using an extended source for experimental analysis. There have also been solutions proposed using rapid refocussing of the telescope, multiple lasers strung around the telescope, wavefront sensors with dynamically steered subapertures, and matched filtering techniques.^{4,5,6,7}

This paper describes a technique of simulating centroid gains from a model which incorporate perspective elongation effects and apply them to an experimental setup. Section 2 discusses the perspective elongation effects that are involved using a laser guide star for adaptive-optics and how the centroid gains using a SH WFS are altered due to those effects. In Section 3 we discuss the AFRL model that was developed which outputs varying centroid gains over different subapertures depending upon the orientation the LGS is launched. In Section 4 the ASALT optical bench layout is presented along with how the model's simulated centroid gains were inserted into that experimental setup. We then present the experiment and conditions using the simulated centroid gains in a closed-loop adaptive-optics system. Section 5 details the results of the experiments. The conclusion of the paper is then given in Section 6.

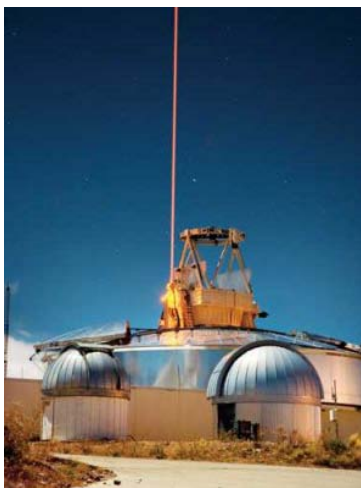


Figure 1. Sodium beacon laser at the Starfire Optical Range.

2. LGS AO

Laser guide stars provide an artificial beacon to measure the atmosphere and provide information for the use of adaptive-optics. The ability to project an LGS in a desired direction, gives the scientific community a means to obtain full sky coverage, rather than using a traditional natural guide star which provides only discrete points to measure the atmosphere. These artificial beacons are created by projecting a laser beam into the upper layers of the atmosphere. Sodium (Na) atoms located in the mesosphere can be used to produce an artificial guide star by tuning the laser to a wavelength of 589 nm causing resonance scattering. The return light from the resonant backward-diffusion of the sodium atoms is then used to measure the turbulent atmosphere. The sodium layer of the atmosphere is concentrated at an altitude of approximately 90 km and has a thickness that ranges from 10-15 km at zenith.⁸ Focusing the laser at these Na atoms creates a column of scattered light due to the finite width of the layer which appears as a circular spot approximately 0.6 arcsec in diameter, though the spot diameter could vary depending on the atmospheric seeing. The image of the beacon from the ground varies depending upon the distance between the launching telescope and the receiving sensor. Beckers performed a detailed analysis of the perspective elongation effect that occurs using a laser guide star.⁹ According to his research, the spot image of the LGS becomes more elongated by approximately 1 arcsec for every 3-4 meters of distance the laser launcher is from the sensor and also depending upon variations in the atmospheric conditions of the sodium layer.

When a SH WFS is used to measure the light from the LGS beacon a lenslet array focuses a different elongated image onto individual subapertures. Each of the individual subapertures have a different perspective angle of the laser beacon causing a variation in the elongation of each spot that a subaperture has focused on its separate quadcell. The subapertures that are located the farthest from the laser launch location have the largest perspective angle causing those spots to be more elongated than subapertures closer to where the laser was launched. Figure 2 is a simulation displaying the focal spots on a SH WFS, where the laser is launched from the center of the aperture. The focal spots become more elongated on the subapertures farthest from the center. The SH WFS computes the local gradients/tilts of the wavefronts with a centroid approximation using a quad cell.

The energy imbalance equation is used in the calculation of the local tilt of the wavefront for each subaperture in the SH WFS. The quadcells of the sensor are composed of four separate pixels A,B,C, and D that correspondingly measure the intensities I_A , I_B , I_C , and I_D as shown in Figure 3. The local wavefront tilt in the subaperture is then computed using the energy imbalance equation as given by

$$s_x = \frac{(I_B - I_A) + (I_D - I_C)}{(I_A + I_B + I_C + I_D)}, \quad (1)$$

$$s_y = \frac{(I_C - I_A) + (I_D - I_B)}{(I_A + I_B + I_C + I_D)}, \quad (2)$$

where s_x and s_y are the transverse slopes. These slopes are multiplied by a calibration factor which takes into account local measured biases.

The measurable tilt over a subaperture is largely dependent upon the width of the spot focused onto the quadcell. The dynamic range of measurable tilt per subaperture is limited by focal spot size because large spots have little available displacement before moving into an adjacent subaperture.¹⁰ Spots need to be fully incident on all four quadrants of the quadcell in order to properly measure the gradient correctly, which is another limit to the dynamic range. Increasing the resolution of the detector array can help mitigate some of these detrimental effects, but this comes at the cost of increasing the read out time and noise effects due to the electronics. Due to the constraints on the spot size, the linear dynamic range of the SH WFS is approximately $\pm\frac{1}{2}$ waves of tilt, which is normally acceptable in closed-loop operation.

The shape of the focal spot is ideally an Airy pattern which gives the same dynamic range of measurable tilt in the x - and y -components. Figure 3 is an example of a radially symmetric focal spot that measures tilt unbiased in the x - and y -components. Asymmetric focal spots have different amounts of dynamic range of measurable tilt with respect to the energy imbalance equation. Figure 5 is an example of an elliptical focal spot that would have a distinctly different y -slope dynamic range as compared to the x -slope due to the focal spot shape illuminated on the quadcell.

Experimental data was taken in the ASALT laboratory to identify the irregular slope measurements in each subaperture from the SH WFS used in this research by dithering the steering mirror in the x - and y -directions and taking open-loop tilt measurements. The reference beam is on-axis similar to Figure 2, thus the center subapertures show symmetric focal spots as compared to the edge subapertures which are more oblong. A center subaperture's measured tilt versus commanded tilt, as shown in Figure 4, has a slope which is generally linear in the ± 0.5 waves of tilt regime, yet begins to saturate beyond that magnitude because the spot is no longer incident on all four quadrants of the quadcell. The centroid gain is the slope within the linear range, which indicates the effective gradient measurement capability of a subaperture. The experimentally measured gradients from an edge subaperture, shown in Figure 6, which has an oblong spot measures tilt differently in the x - and y -directions. The discrepancy in how the x - and y -components measure tilt causes errors in the determination of the resultant slope and subsequent reconstructed phase. These discrepancies in the slope measurements are inherent in an AO system using a SH WFS, but are accentuated using an extended source which is represented in the AFRL spot model.

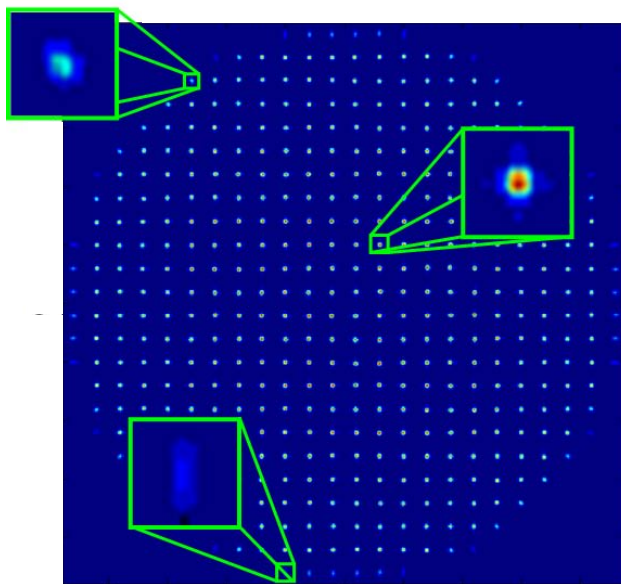


Figure 2. Images of focal spots on a SH WFS with an on-axis reference beam. Center subapertures near the on-axis reference beam have symmetrical focal spots. Edge subapertures that are farther from the center are elongated.

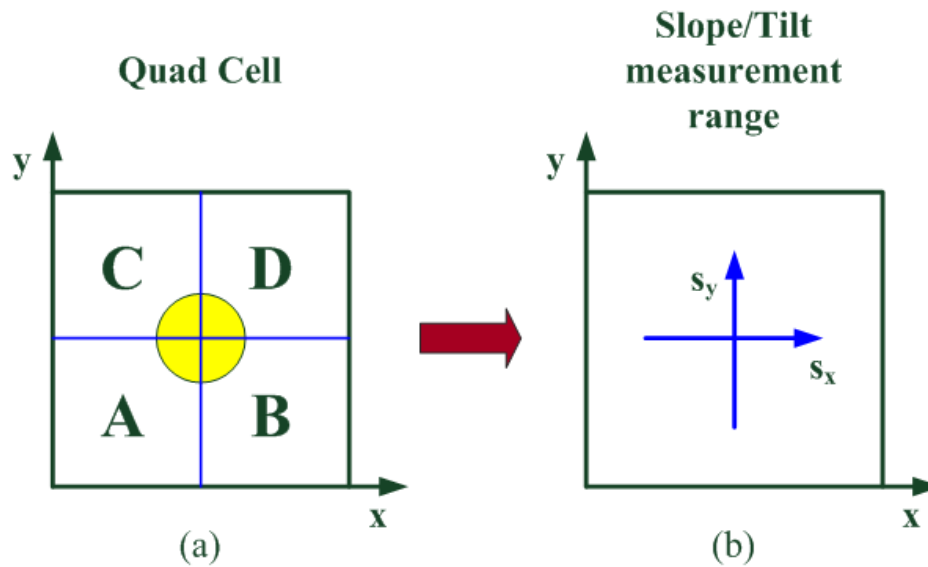


Figure 3. Quad cell and radially symmetric focal spot. (a) Quad cell with centered focal spot. (b) Similar slope measurement ranges in the x and y component.

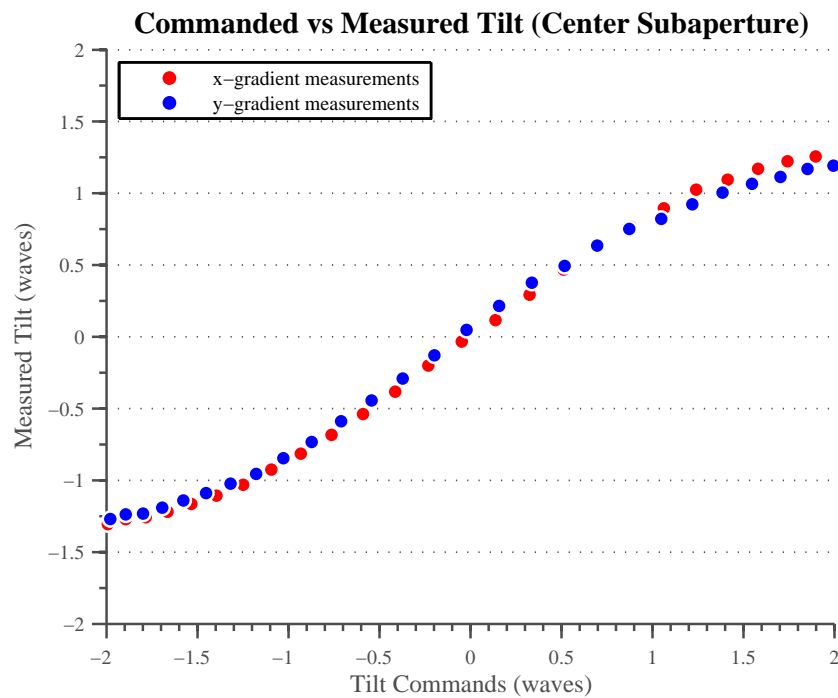


Figure 4. Gradient response for a fully illuminated focal spot on a center subaperture. The x and y gradient have similar slope/centroid gains due to a radially symmetric centroid.

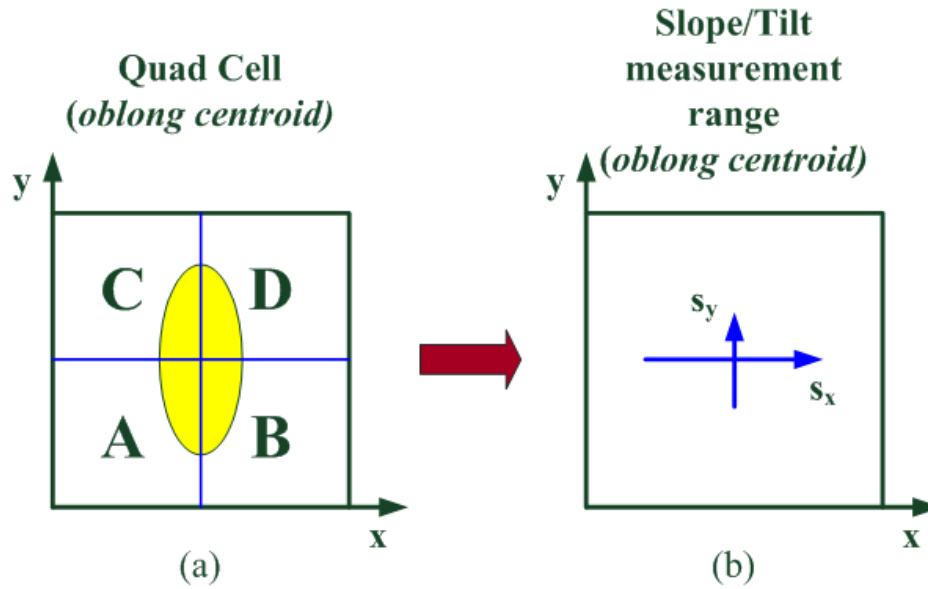


Figure 5. Quad cell and elongated focal spot. (a) Quad Cell with asymmetrical focal spot. (b) Different slope measurement ranges in the x and y component.

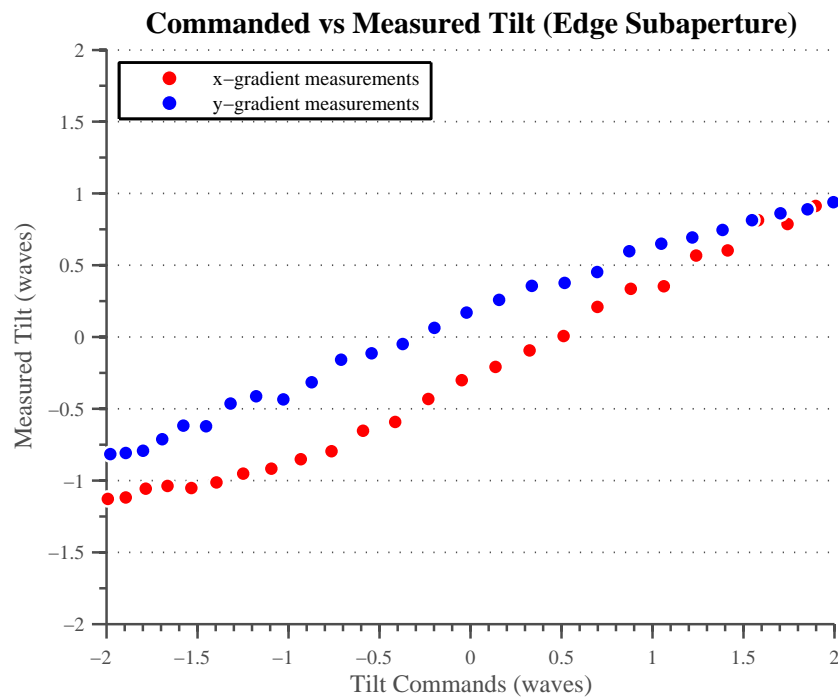


Figure 6. Gradient response for an elongated focal spot on an edge subaperture. The y gradient response has a lower slope/centroid gain due to elongation in the centroid which causes a lower dynamical range of measurability. There are also bias offsets in the response due to the position of the focal spot when there is no commanded tilt.

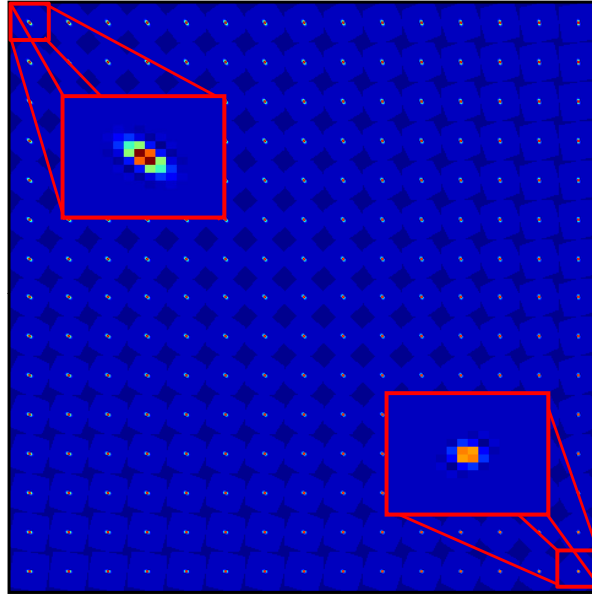


Figure 7. Spot Model: Spot Image Example

3. LGS SPOT MODEL

A LGS spot model was developed to update the references for the LGS WFS on the Sodium Guidestar Adaptive Optics for Space Situational Awareness Program's (NGAS) AO system at the SOR.¹ The model updates the reference by determining the null offsets and gains for subapertures of the WFS based on their specific geometric orientation to the laser launch position of the Na beacon. An elliptical Gaussian model is used to model the shape of each spot, S , on a SH WFS using the direction and location the beacon is pointed, as shown by,

$$S(x, y; \theta_M) = \exp \left[-\frac{x^2}{(L_M + w_{st})^2} - \frac{y^2}{w_{st}^2} \right], \quad (3)$$

where (x, y) is the position of a given subaperture, θ_M is the orientation of the major axis of the spot, L_M is the geometric length to the beacon, and w_{st} is the beam radius. The strength of the atmospheric turbulence represented by Fried's parameter, r_0 , and the wavelength of the laser beacon vary the radius, w_{st} , of the Gaussian profile of the beam.

An example of the varied images from the spot model are shown in Figure 7. The laser beacon is launched from the lower right corner of the aperture and the shape of the focal spots reflect that geometry, with more elongation on the spots farthest away from the laser launch location. The different elliptical shapes of the spots alter the gradient measurement effectiveness in each subaperture, as mentioned in Section 2. The model represents the changes in the gradient measurement capability by computing centroid gains in the x - and y -components for each subaperture. Figure 8 are the x - and y - component centroid gains for the calculated focal spots shown in Figure 7. The gains in the example range from values of 1 to 0.6, which go from extremes of normal gradient measurability to a decrease in the gain due to elongation representing the lowering of dynamic range in the extended component axis, respectively. A centroid gain of 1 is normalized in each component and is representative of a symmetric focal spot. The lower-right region which is near the laser launch location have centroid gain values that are closer to 1 due to the geometric considerations. Correspondingly, the subapertures that are farthest away from the laser launch location have degraded measurability which is shown in the centroid gains which are less than 1.

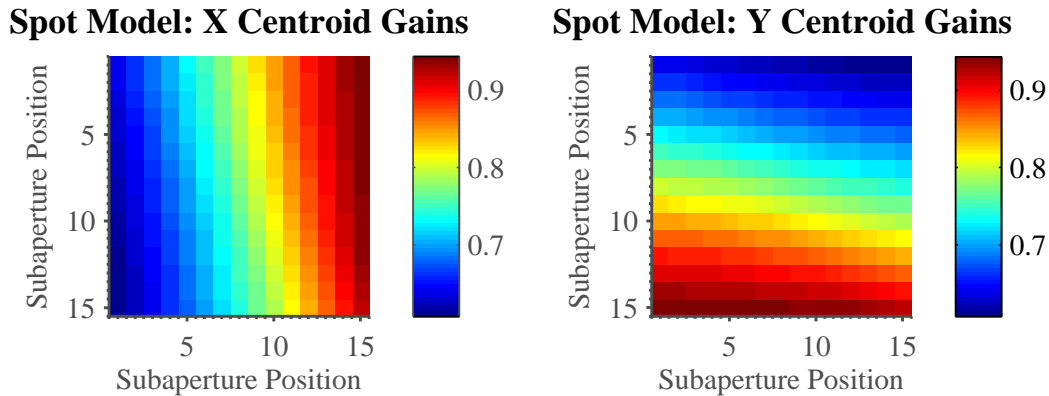


Figure 8. Spot Model: Gains Example

4. EXPERIMENTAL SETUP

The ASALT is particularly well-suited for this research because it allows for repeatable experiments under different turbulence conditions and is in a well-controlled environment. The optical bench described in Section 4.1 and its corresponding hardware is controlled by a computer console which computes all of the data processes in the AO system. This console allows for programmable processing scripts to be inserted in the data flow of the AO system, giving the ability to apply the model's simulated centroid gains directly to the experimental setup, as described in Section 4.2.

4.1 Laboratory bench setup

A layout of the bench and its optics is given in Figure 9. The beam path on the optical table begins with a 1550 nm laser as the source. The beam is propagated through the atmospheric turbulence simulator (ATS) consisting of two phase wheels that are used to simulate the atmospheric conditions, which can be controlled. The aberrated beam is then reflected off a steering mirror (SM) to compensate for the tilt/tip in the beam. The DM then applies a high-order correction to the beam and is controlled by the DM controller. After reflecting off the DM, the beam is then projected through a set of beamsplitters to the SH WFS and self-referencing interferometer (SRI). The SRI is a WFS that can directly measure the phase, but in this research the SH WFS will be used to close the loop. The beam is focused and readjusted with the optics within this process to simulate a 1.5 meter AO system, though it also can be scaled to simulate other telescope sizes.

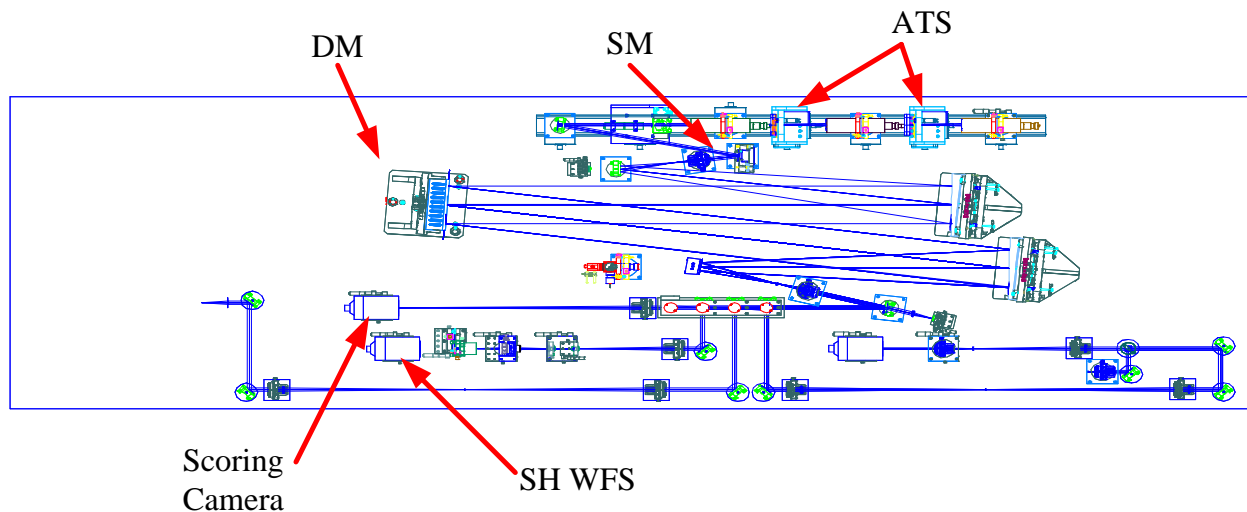


Figure 9. ASALT optical table layout in SRI-2.¹¹

Table 1. Experiment Parameters: $\Delta 5$ is change in 5 degrees for each data set

Test Set	r0(cm)	Rytov	Elev. Angle (degrees)	Laser Dist.(m)
1	10.5	0.580	1-89, $\Delta 5$	3.29
2	12.7	0.092	1-89, $\Delta 5$	3.29
3	14.2	0.002	1-89, $\Delta 5$	3.29

4.2 Perspective elongation gain application

The normalized centroid gains developed by the LGS spot model are directly multiplied by the gradient measurements from the SH WFS to incorporate the simulated effects of spot elongation to the AO system. The gain induced gradient measurements are then reconstructed into phase space and filtered to produce the commands to the DM. Table 1 shows the different turbulence conditions that were simulated using the ATS, as well as the geometric conditions used to produce the centroid gains. The azimuth angle for each set of gains was similar for all experiments to specifically analyze the elongation due to the elevation angle. Elevation angles for each turbulence condition were varied from ≈ 89 degrees to 1 degree, which correspond to pointing straight up near zenith to pointing almost horizontally, respectively.

5. RESULTS AND ANALYSIS

The gains corresponding to the elevation angles used in Table 1 were incorporated onto the SH WFS to analyze the effects perspective elongation has on the performance of an AO system. The focal spots on the subapertures became more elongated as the elevation angle deviated from zenith, which were represented in the calculated centroid gains from the model. The subapertures that had the most elongated spots also had lower corresponding gains in the major axis of the elliptical focal spot. The gradient measurements in these particular subapertures were degraded due to the simulated elongation of the focal spot.

The normalized gradient variance was calculated on each set of data to spatially visualize the degradation of the gradient measurements due to elongated spots. The sets of experiments that used the model with elevation angles near zenith outputted centroid gains to ≈ 1 in each axis to reflect the negligible effects of perspective elongation. The gradient variance on the subapertures were generally uniform in these conditions near zenith. Though in contrast, the conditions where the model was set to lower elevation angles showed a strong relationship between simulated elongated focal spots and corresponding gradient variance in those subapertures. Figure 10 show the centroid gains for a turbulence condition of $r_0 = 14.2$ cm and an elevation angle of 30 degrees. The corresponding x - and y - gradient variances are shown in Figures 11 and 12. The gradient variances in each of these figures are directly related to the centroid gains applied to the SH WFS. Subapertures that have lower centroid gains simulating elongation have larger gradient variances in the corresponding axis due to the degradation in the measurable dynamic range.

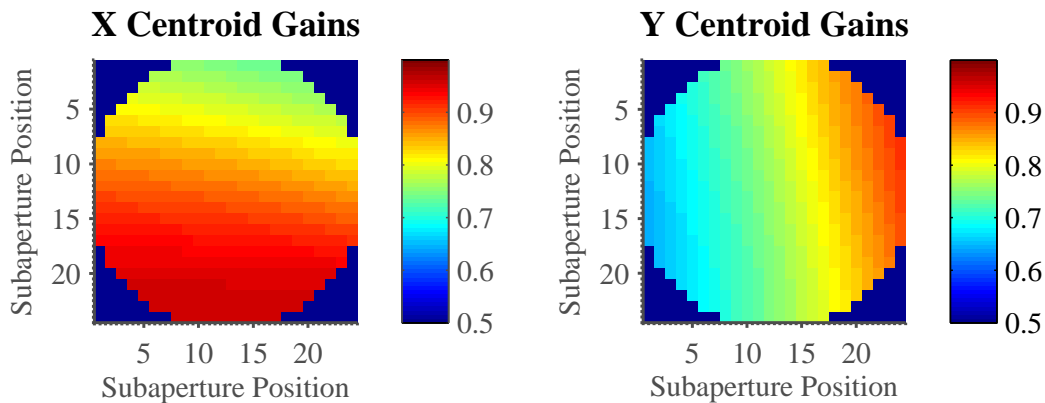


Figure 10. Centroid Gains ($r_0 = 14.2$ cm, Elevation Angle = 30 degrees)

X Gradient Variance ($r_0 = 14.2$ cm, Elev. $\angle = 30^\circ$, normalized)

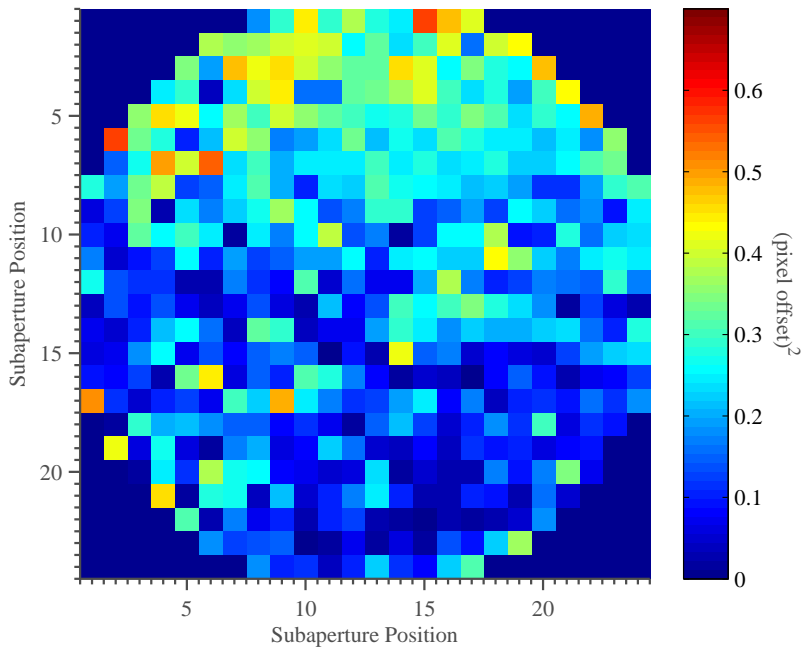


Figure 11. Normalized X Gradient Variances ($r_0 = 14.2$ cm, Elevation Angle = 30 degrees)

Y Gradient Variance ($r_0 = 14.2$ cm, Elev. $\angle = 30^\circ$, normalized)

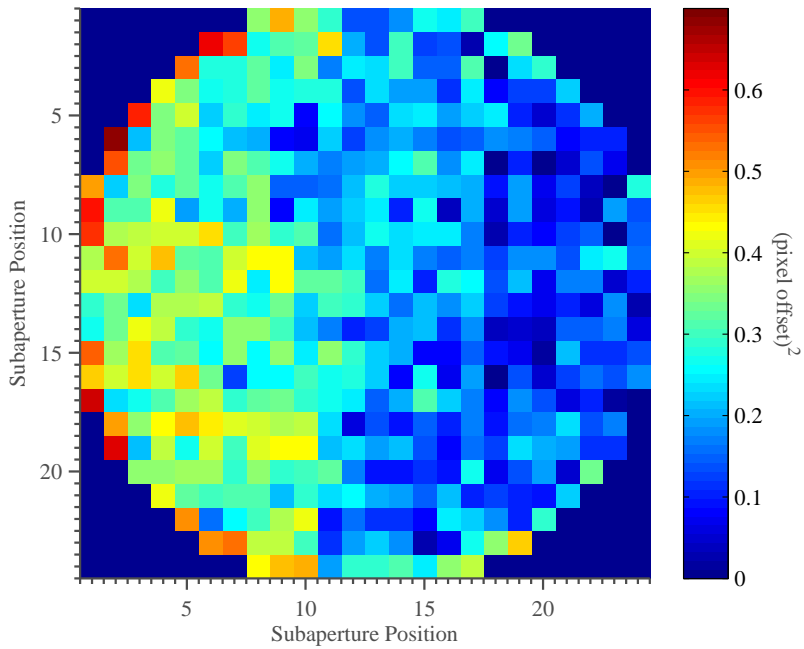


Figure 12. Normalized Y Gradient Variances ($r_0 = 14.2$ cm, Elevation Angle = 30 degrees)

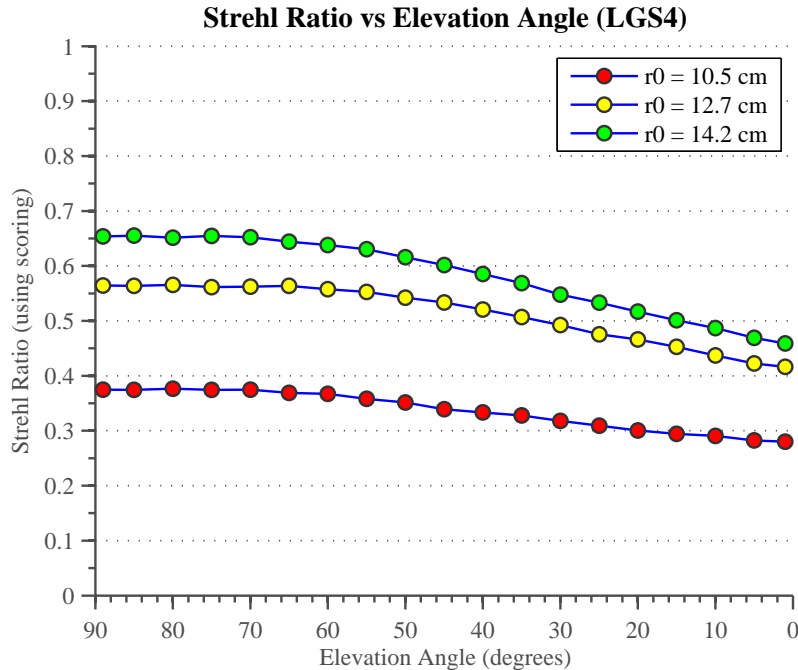


Figure 13. Strehl vs Elevation Angle

The metric used for the performance of the closed-loop AO system was the Strehl ratio, which was determined using a power-in-the-bucket calculation of the compensated point source. The Strehl ratio was recorded at different elevation angles for each turbulence condition, as shown in Figure 13. Each set of turbulence conditions showed a degradation in Strehl with corresponding lower elevation angles due to the effects of simulated perspective elongation. The overall gradient variance in each set of data increased as the elevation lowered which directly degraded the AO performance. The turbulence condition was not changed with elevation angle in order to separately analyze the elongation effects from the model.

6. CONCLUSION

The application of centroid gains to the SH WFS allows modeled perspective elongation effects to be incorporated onto an optical test bench without altering the associated hardware. This was a preliminary exploration into the aberrations caused by using LGS beacons, in preparation for the insertion of an extended beacon in the ASALT laboratory. The centroid gains from the model effectively degraded the gradient measurement capability in the axes of simulated elongated focal spots. Future research in the ASALT laboratory is planned for developing new techniques to mitigate for the effects of perspective elongation using LGS beacons, as well as explore established methods that are currently used in the field.

ACKNOWLEDGMENTS

We would like to thank the Air Force Office of Scientific Research for their support in funding this research.

REFERENCES

- [1] Roskey, D. and Olikier, M., "Lgs spot model for ngas wavefront sensor referencing," tech. rep., Air Force Research Laboratory, Starfire Optical Range (2008).
- [2] Vitayaudom, K. P., Vincent, T. R., Schmidt, J. D., and Sanchez, D. J., "Analysis of non-uniform gain for control of a deformable mirror in an adaptive-optics system," **7093**, SPIE (2008).
- [3] Véran, J. and Herriot, G., "Centroid gain compensation in shack-hartmann adaptive optics systems with natural or laser guide star," *J. Opt. Soc. Am. A* **17**(8), 1430–1439 (2000).

- [4] Beckers, J. M., Owner-Peterson, M., and Andersen, T., "Rapid refocusing system for the euro50 telescope aimed at removing the perspective elongation of laser beacons," **5169**, SPIE (2003).
- [5] Ribak, E. N. and Ragazzoni, R., "Reduction of laser spot elongation in adaptive optics," *Opt. Lett.* **29**(12), 1351–1353 (2004).
- [6] Baranec, C., Bauman, B. J., and Lloyd-Hart, M., "Concept for a laser guide beacon shack-hartmann wavefront sensor with dynamically steered subapertures," *Opt. Lett.* **30**(7), 693–695 (2005).
- [7] Conan, R., Lardiere, O., Herriot, G., Bradley, C., and Jackson, K., "Experimental assessment of the matched filter for laser guide star wavefront sensing," *Appl. Opt.* **48**(6), 1198–1211 (2009).
- [8] Viard, E., Delplancke, F., Hubin, N., and Ageorges, N., "Lgs na-spot elongation and rayleigh scattering effects on shack-hartmann wavefront sensor performances," **3762**, SPIE (1999).
- [9] Beckers, J. M., "Removing perspective elongation effects in laser guide stars and their use in the eso very large telescope," *Progress in telescope and Instrumentation Technologies* (1992).
- [10] Plett, M. L., Barbier, P. R., Rush, D. W., Polak-Dingels, P., and Levine, B. M., "Measurement error for a shack-hartmann wavefront sensor in strong scintillation conditions," **3433**, SPIE (1998).
- [11] Rhoadarmer, T., "Wave front sensors and basic reconstruction," Briefing at AFRL. (March 2002).

DISTRIBUTION LIST

DTIC/OCP 8725 John J. Kingman Rd, Suite 0944 Ft Belvoir, VA 22060-6218	1 cy
AFRL/RVIL Kirtland AFB, NM 87117-5776	2 cy
Patrick Kelly Official Record Copy AFRL/RDSA	1 cy